Robotics: Science and Systems 2023
Daegu, Republic of Korea, July 10-July 14, 2023

StructDiffusion: Language-Guided Creation of Physically-Valid Structures using Unseen Objects

Weiyu Liu[1], Yilun Du[2], Tucker Hermans[3], Sonia Chernova[1], Chris Paxton[4]

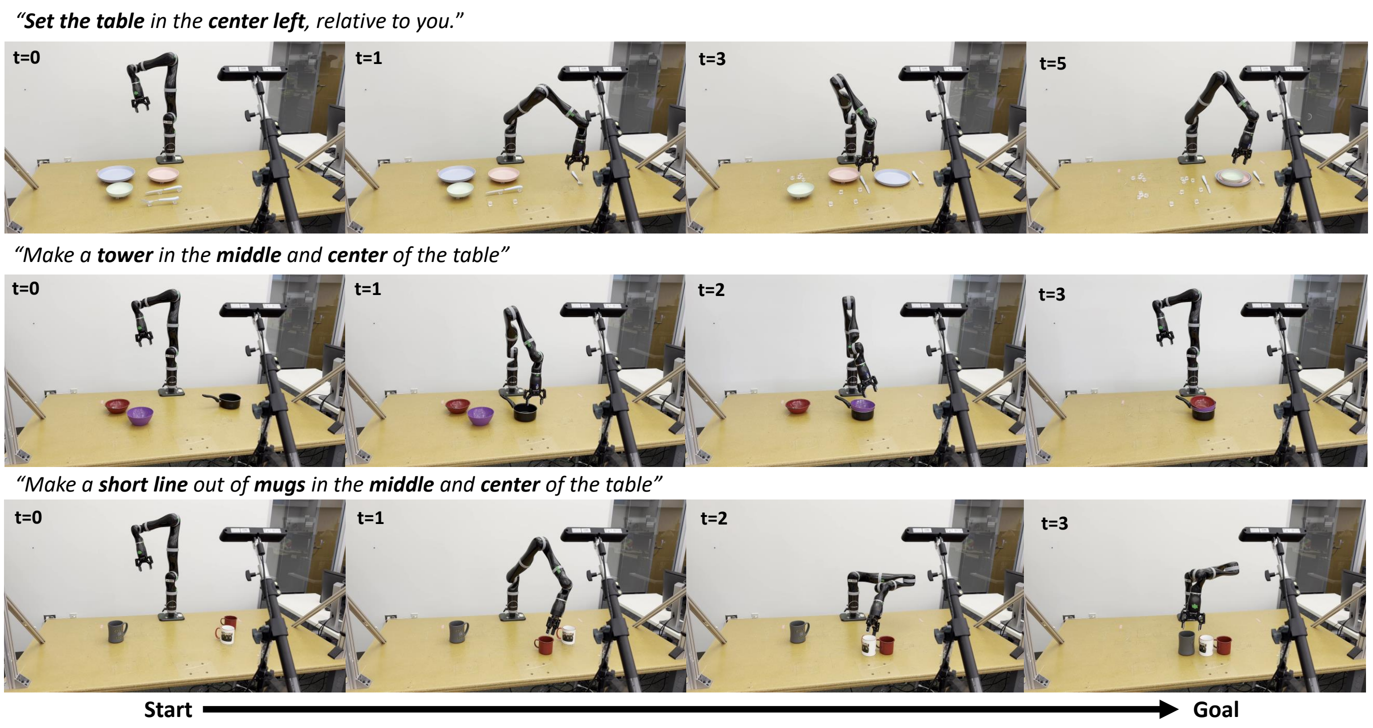
"Set the table in the center left, relative to you."
t=0
t=1
t=3
t=5
"Make a tower in the middle and center of the table"
t=0
t=1
t=2
t=3
"Make a short line out of mugs in the middle and center of the table"
t=0
t=1
t=2
t=3
Start
Goal

Fig. 1: Real-world rearrangement with unseen objects, given a language instruction. We use StructDiffusion to predict possible goals that satisfy physical constraints such as avoiding collisions between objects. At the core of StructDiffusion is an object-centric multimodal transformer backbone combined with a diffusion model, capable of sampling diverse high-level motion goals for language-guided rearrangement.

***Abstract*—Robots operating in human environments must be able to rearrange objects into semantically-meaningful configurations, even if these objects are previously unseen. In this work, we focus on the problem of building physically-valid structures without step-by-step instructions. We propose StructDiffusion, which combines a diffusion model and an object-centric transformer to construct structures given partial-view point clouds and high-level language goals, such as "set the table". Our method can perform multiple challenging language-conditioned multi-step 3D planning tasks using one model. StructDiffusion even improves the success rate of assembling physically-valid structures out of unseen objects by on average 16% over an existing multi-modal transformer model trained on specific structures. We show experiments on held-out objects in both simulation and on real-world rearrangement tasks. Importantly, we show how integrating both a diffusion model and a collision-discriminator model allows for improved generalization over other methods when rearranging previously-unseen objects. For videos and additional results, see our website: https://structdiffusion.github.io/.**

I. Introduction

Structures are everywhere in the real world: shelves are stocked, tables are set, furniture is assembled. For robots to be successful assistants and collaborators, they must understand object structures and build these structures based on human commands. In this work, we predict how previously-unseen objects should be rearranged in order to realize language instructions, given only partial-view point cloud of a scene. Solving this task requires models that can reason about different constraints over where objects should be at once (e.g., object geometry, language-driven task semantics, physics) and generate solutions that respect all these constraints.

Assume a robot is given a language instruction such as "set the table." First, the objects must in the correct relative positions in order to satisfy desired spatial and semantic relations: utensils on the sides, plate in the center, for example. Second, arrangements must be physically valid: even if the plate is bigger than the robot saw in training data, it should not collide with the utensils. These constraints correspond to two overlapping, but not identical, sets of possible solutions where a robot can place objects.

One potential approach for this task is to train a language-conditioned multi-modal transformer to directly predict the best sequence of actions the robot should take [1, 2, 3, 4, 5].

[1]Georgia Tech, [2]MIT, [3]University of Utah and NVIDIA, [4]Meta AI

Such models have achieved impressive results on pick-and-place tasks for known objects [1, 3]; however, for structure generation of unseen objects, regressing to a single solution can often create problems when there are multiple, potentially conflicting, constraints (e.g., place objects "tightly" but avoid collisions) [4]. By contrast, planning-inspired approaches work by generating and refining a distribution over estimated poses [6], most notably diffusion models [7, 8]. Such diffusion models have shown applications not just to image generation [9, 10, 11, 12], but to motion planning and pose estimation [8, 7], and to rearrangement [12], achieving better results than previous policies due to their ability to more accurately capture the space of potential solutions.

We hypothesize that by iteratively refining predicted goals from a diffusion model, subject to learned constraints, we can similarly find better solutions for language-conditioned structure creation. In our approach, called *StructDiffusion*, we first use unknown object instance segmentation to break up our scene into objects, as per prior work [6, 13, 14, 15]. Then, we use a multi-modal transformer to combine both word tokens and object encodings from Point Cloud Transformer [16] in order to make 6-DoF goal pose predictions. These predictions are both refined iteratively via diffusion and the best goal is selected with a *discriminator* model that is trained to recognize unrealistic samples. Because goals are predicted relative to the observed partial-view point clouds of the objects, it's possible to get strong results without any object models or object foreknowledge. We train two main components:

1) **An object-centric, language-conditioned diffusion model**, which learns how to construct different types of multi-object structures from observations of novel objects and language instructions.
2) **A learned discriminator**, which drastically improves performance by rejecting samples violating physical constraints.

This approach allows *StructDiffusion* to resolve problems not possible in previous work. Compared to an existing single-task model and a strong multi-task baseline we introduce, *StructDiffusion* achieves 16.3% and 13.5% higher success rates respectively. To our knowledge, *StructDiffusion* is the first work that can build multiple structures requiring stacking and 3D reasoning, while generalizing over different unseen objects given high-level language instructions. We believe that this approach will allow for language-guided control of robots, to be applied to more complex tasks and environments.

II. Related Work

Language-conditioned manipulation is a fast-growing area of research [2, 17, 4, 3, 18, 19, 20]. Recently. Say-Can [21] showed how a large language model (LLM) can be used to sequence robot skills to respond to a wide range of natural-language queries. This work has been extended to use a map and object-centric representation of the world [22]. As this line of work leverages LLMs for reasoning, they use a purely language-based version of the world and require efforts in prompt engineering [13, 23, 21]. Another thread of work looks more closely at learning language-conditioned skills, and has achieved impressive results on a variety of pick-and-place and articulated object manipulation tasks [2, 18, 3]; however, these approaches yet to demonstrate whether the skills can be sequenced to create more complex structures we study here. It's worth noting that several of these works have used an object-centric representation of the world [1, 22, 4], where objects are first segmented or detected and then encoded separately. For example, VIMA [1] used encoded object patches as input to a multimodal transformer. These works, however, do not look specifically at generating *physically realistic* structures: in our experiments, we show how these direct-regression-first approaches do not generate the same quality of structures, and that, in particular, simply predicting the best placement poses or actions will lead to more failures.

Our work is related to planning with unknown objects. Simeonov et al. [24] propose a planning framework for rigid objects, but they do not study structures with complex dependencies. Curtis et al. [25] investigate task and motion planning with unknown objects, which relies on a similar segmentation and grasping pipeline we use, but does not look at learning goals, instead assume access to a set of predicates (e.g., Red, on) which can be evaluated at planning time.

Furthermore, there is a set of works which learn object-object relations for planning [6, 26, 27, 28], which is relevant to our method's refinement process. Many of these do so explicitly. In particular, learning object skill preconditions is very useful for sequential manipulation, so some works look at predicting relationships in this context [29, 27, 30]. For example, SORNet [27] learns to predict relations between objects given a canonical image view of the objects; similarly a predictive model from image inputs is learned for capturing relationships [30]. These object-object relations are an important part of planning sequential manipulation as per *StructDiffusion*, but we pay attention to implicitly classifying object relationships as a whole.

Finally, a set of recent works have explored how diffusion models may be applied to robotics [7, 31, 8, 12, 32]. In [7, 31, 32], the diffusion model is used to parameterize the motion planning procedure, while our approach focuses on generating rearrangement goals for manipulation. Furthermore, these works require known object models and are not conditioned on flexible language goals. Similar to our work, in DALL-E-Bot [12], DALL-E is used to generate a goal image for an arrangement of multiple objects, from which object matching is used to obtain an rearrangement of objects. However, this approach assumes that underlying state of world can be captured using an overhead image, as a generated image is used to parameterize the final goal and a motion plan. In our case, we directly generate object placement poses given point cloud observations, and are thus unrestricted by which position or angle the image is generated from.

III. Preliminaries

We provide background information on diffusion models [10, 11] and transformers [33]. These two neural network

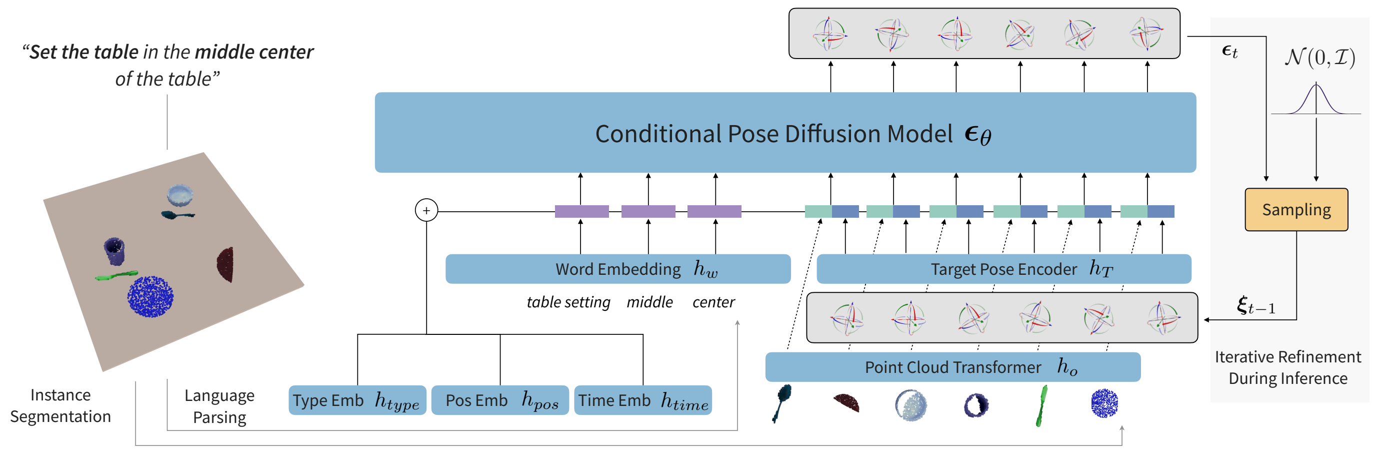
"Set the table in the middle center of the table"
Instance Segmentation
Language Parsing
Type Emb h_{type}
Pos Emb h_{pos}
Time Emb h_{time}
Word Embedding h_w
table setting
middle
center
Target Pose Encoder h_T
Point Cloud Transformer h_o
Conditional Pose Diffusion Model ϵ_θ
ϵ_t
$\mathcal{N}(0, \mathcal{I})$
Sampling
ξ_{t-1}
Iterative Refinement During Inference

Fig. 2: Overview of the object-centric diffusion model. We combine a diffusion model with an object-centric multimodal transformer to iteratively reason about both 3D object embeddings and task specification in language, and to predict goal poses of objects.

structures provide core components for our approach.

A. *Diffusion Models*

Denoising Diffusion Models are a class of generative models [10, 11]. Given a sample $x \sim q(x_0)$ from the data distribution. The *forward* diffusion process is a Markov chain that creates latent variables $x_1, ..., x_T$ by gradually adding Gaussian noise to the sample:

$$q(x_t|x_{t-1}) = \mathcal{N}(x_t; \sqrt{1-\beta_t}x_{t-1}, \beta_t\mathcal{I})$$

Here β_t follows a fixed variance schedule such that the variance at each step is small and the total noise added to the original sample in the chain is large. These two conditions allows sampling $x_0 \sim p_\theta(x_0)$ from a *reverse* process that starts with a Gaussian noise x_T and follows a learned Gaussian posterior

$$p_\theta(x_{t-1}|x_t) \sim \mathcal{N}(x_{t-1}; \mu_\theta(x_t, t), \Sigma_\theta(x_t, t))$$

In this work, we adopt the simplified model introduced in [11] that fixes the covariance $\Sigma_\theta(x_t, t)$ to an untrained time-dependent constant and reparameterize the mean $\mu_\theta(x_t, t)$ with a noise term ϵ_t. Diffusion models can be trained to minimize the variational lower bound on the negative log-likelihood $\mathbb{E}[-\log p_\theta(x_0)]$. A simplied training objective with the reparameterized mean can be derived as:

$$L_{\text{simple}} = \mathbb{E}_{t\sim[1,T], x_0\sim q(x_0), \epsilon\sim\mathcal{N}(0,\mathcal{I})}[||\epsilon - \epsilon_\theta(x_t, t)||^2]$$

B. *Transformers*

Transformers were proposed in [33] for modeling sequential data. At the heart of the Transformer architecture is the scaled dot-product attention function, which allows elements in a sequence to attend to other elements. Specifically, an attention function takes in an input sequence $\{x_1, ..., x_n\}$ and outputs a sequence of the same length $\{y_1, ..., y_n\}$. Each input x_i is linearly projected to a query q_i, key k_i, and value v_i. The output y_i is computed as a weighted sum of the values, where the weight assigned to each value is based on the compatibility of the query with the corresponding key. In this work, we use the encoder layers in the original transformer architecture. Each encoder layer includes an attention layer and a position-wise fully connected feed forward network. With the use of attention mask, the encoder layer can process sequences with different lengths.

IV. *StructDiffusion* for Object Rearrangement

Given a single view of an initial scene containing objects $\{o_1, ..., o_N\}$ and a language specification containing word tokens $\{w_1, ..., w_M\}$, our goal is to rearrange the objects into a goal configuration that satisfies the language goal. We assume the objects are rigid and we are given a partial-view point cloud of the scene with segment labels for points to identify the objects. We can extract the initial poses of the objects $\{\xi_1^{pc}, ..., \xi_N^{pc}\}$ from the segmented object point clouds $\{x_1, ..., x_N\}$ by setting the rotation to zero and the position to the centroid of each object point cloud in the world frame. To rearrange the objects, the robot needs to move each object to ξ_i^{goal}, which is the goal pose in the world frame defined for the point cloud of the i-th object

In this work, our robot can execute pick and place actions. For each object, we can sample a set of stable grasps $\mathcal{G} = \{g_1, ..., g_J\}$. Given a target pose for object ξ_i^{goal} and a stable grasp g_j, the robot can move its end effector to $\xi_i^{ee} = \xi_i^{goal}(\xi_i^{pc})^{-1}g_j$ to place the object at the goal pose. We only use pick and place actions in our setup to simplify the problem. However, our object-centric actions can be integrated with sampling-based TAMP solutions [25] to also leverage other motion primitives, such as pushing and regrasping, to reach the goal poses predicted by our system.

Below, we describe our approach for sampling goal poses for objects based on partial point clouds, given a language goal. Our framework combines a generator based on a diffusion model and a learned discriminator that filters out invalid samples. As shown in Fig. 2, our diffusion model is integrated with a transformer model that maintains an individual attention stream for each object. This object-centric approach allows us to focus on learning the interactions between objects based on their geometric features, as well as the grounding of abstract concepts on spatio-semantic relations between objects

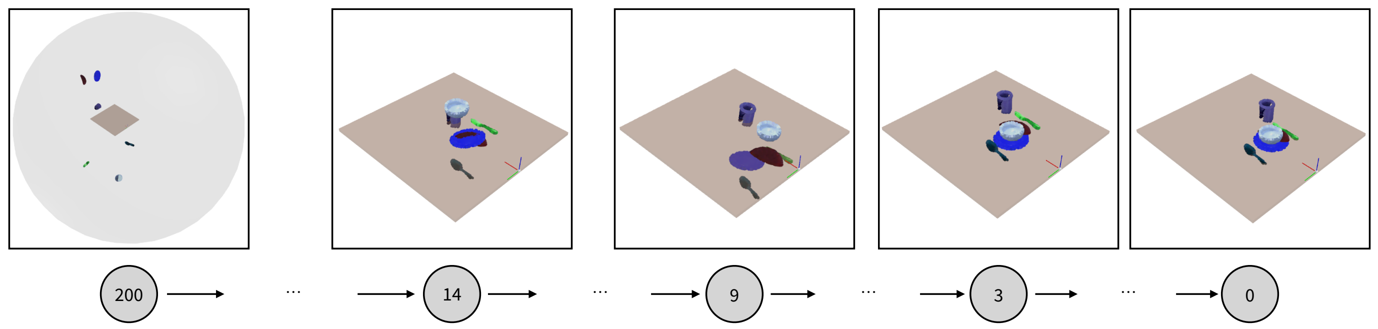

Fig. 3: We model goal generation for semantic rearrangement as a diffusion process. For each sample, we start from the last step of the reverse diffusion process, which places objects randomly in space, and jointly predict goal poses for all objects in the scene. This formulation allows our model to reason about object-object interactions in a generalizable way, which outperforms simply predicting goal poses from multi-modal inputs.

(e.g., large, circle, top). The discriminator model operates on the imagined scene after transforming the objects to their predicted goal poses to further reject invalid samples. Below, we introduce the generator in Sec. IV-A and Sec. IV-B and the discriminator in Sec. IV-C.

A. *Encoders*

We leverage modality-specific encoders to convert the multimodal inputs to latent tokens that are later processed by the transformer network.

Object encoder. Given the segmented point cloud x_i of an object o_i, we use a learned encoder $h_o(x_i)$ to encode each object separately. This encoder uses the Point Cloud Transformer (PCT) [16] to process the centered object point cloud, which has been shown to be effective at shape classification and part segmentation. The mean position of the original object point cloud before centering is encoded using a multilayer perceptron (MLP). Encodings from the two networks are concatenated to give the latent representation for each object $h_o(x_i)$, which we use for semantic, geometric, and spatial reasoning. Separately encoding the geometry and position allows the latent representation to be translationally invariant.

Language. We encode specific word tokens that can indicate the class, position, orientation, and size of the target structure from the language instruction, following prior work [4]. We map each unique word token separately to an embedding with a learned mapping $h_w(w_i)$. This method helps establish a fine-grained correspondence between each part of the language specification and the respective constraint on the generated structure. In Appendix A, we explore two more language encoding options: encoding natural language sentences directly, and using large language models (LLMs) to map sentences to the domain-specific word tokens (e.g., mapping "putting objects far apart" to "large" for the size of the structure).

Diffusion encodings. Since the goal poses of objects are iteratively optimized by the diffusion model and need to feed back to the model during sampling, we use a MLP to encode the goal poses of the objects $h_T(\xi_i^{goal})$. To compute the time-dependent Gaussian posterior for reverse diffusion, we combine a latent code for t in the feature channel by learning a time embedding $h_{time}(t)$.

Positional encoding. To differentiate the multimodal data and objects, we use a learned position embedding $h_{pos}(i)$ to indicate the position of the words and objects in input sequences and a learned type embedding $h_{type}(\upsilon_i)$ to differentiate object point clouds ($\upsilon_i = 1$) and word tokens ($\upsilon_i = 0$).

B. *Conditional Pose Diffusion Model*

Combining a diffusion model and an object-centric transformer, *StructDiffusion* can sample diverse yet realistic object structures while accounting for the complex constraints imposed by the object geometry and language goal. The conditional diffusion model predicts the goal poses for the objects $\boldsymbol{\xi}_0 = \{\xi_i\}_i^N$ starting from the last time step of the reverse diffusion process $\boldsymbol{\xi}_T \sim \mathcal{N}(0, \mathcal{I})$, which is a multivariate normal distribution with independent components. We use the bold symbol here because we jointly optimize the poses of all objects. The reverse diffusion process is illustrated in Fig. 3.

Object-centric transformer. Different from most existing diffusion models that directly generate goal images and do not explicitly model individual objects [9, 10, 11, 12], we use the transformer model to build an object-centric representation of the scene and reason about the higher-order interactions between multiple objects. This approach allows us to account for both global constraints and local interactions between objects. Leveraging attention masks, a single transformer model can also learn to rearrange different numbers of objects.

Diffusion. The use of the diffusion model helps us capture diverse structures since we are sampling from a series of Gaussian noises at different scales when going from $\boldsymbol{\xi}_T$ to our goal $\boldsymbol{\xi}_0$. The resulting samples, therefore, is diverse at different levels of granularity (e.g., different placements of the structures and different orientations of the individual objects). Diversity is also crucial when dealing with the inherent ambiguity in language instructions. For example, a *large* circle of plates and a *large* circle of candles impose different constraints on the proportions of the structures because the objects being arranged have different sizes.

Combining the advantages of the object-centric transformer and the diffusion model, we propose to model the conditional

Algorithm 1 Goal generation with *StructDiffusion*

```
1: for $t \in \text{range}(T, 1)$ do
2:     $\boldsymbol{\epsilon}_t \sim \boldsymbol{\epsilon}_\theta(\boldsymbol{\xi}_t, t, \{x_i\}, \{w_i\})$
3:     $\boldsymbol{z} \sim \mathcal{N}(0, \mathcal{I})$ if $t > 1$ else $\boldsymbol{z} = 0$
4:     $\boldsymbol{\xi}_{t-1} = \frac{1}{\sqrt{\beta_t}}(\boldsymbol{\xi}_t - \frac{\beta_t}{\sum_{s=1}^{t} 1-\beta_t}\boldsymbol{\epsilon}_t) + \sqrt{\beta_t}\boldsymbol{z}$
5: Transform object points: $x_i^{goal} = \xi_i^{goal}(\xi_i^{pc})^{-1}x_i$
6: Compute discriminator scores
7: return ranked $\boldsymbol{\xi}_0$
```

reverse process as

$$p_\theta(\boldsymbol{\xi}_0|\{x_i\}, \{w_i\}) = p(\boldsymbol{\xi}_t)\prod p_\theta(\boldsymbol{\xi}_{t-1}|\boldsymbol{\xi}_t, \{x_i\}, \{w_i\})$$

The generation process depends on the point clouds of the objects and language instruction. As discussed in III-A, we learn the time-dependent noise $\boldsymbol{\epsilon}_t$, which can be used to compute $\boldsymbol{\xi}_t$. We use the transformer as the backbone to predict the conditional noise $\boldsymbol{\epsilon}_\theta(\boldsymbol{\xi}_t, t, \{x_i\}, \{w_i\})$ for each object. We obtain the transformer input for the language part c and the object part e as

$$c_{i,t} = [h_w(x_i); h_{pos}(i); h_{type}(v_i); h_{time}(t)]$$
$$e_{i,t} = [h_o(x_i); h_T(\xi_i^{goal}); h_{pos}(i); h_{type}(v_i); h_{time}(t)]$$

where $[;]$ is the concatenation at the feature dimension. The model takes in the sequence $\{c_{1,t}, .., c_{M,t}, e_{1,t}, ..., e_{N,t}\}$ and predicts $\{\epsilon_{1,t}, ..., \epsilon_{N,t}\}$ for the object poses[1]. We parameterize 6-DoF pose target ξ as $(t, R) \in SE(3)$. We directly predict $t \in \mathbb{R}^3$ and predict two vectors $a, b \in \mathbb{R}^3$, which are used to construct the rotation matrix $R \in SO(3)$ using a Gram–Schmidt-like process proposed in [34].

C. Discriminators

In addition to the generator, we also use a learned discriminator model to further filter the predictions for realism, given only partial point cloud observation. The discriminator works on imagined scenes, where the point clouds of objects are rigidly transformed to the respective goal poses following $x_i^{goal} = \xi_i^{goal}(\xi_i^{pc})^{-1}x_i$. As the discriminator is trained to predict a score $s \in [0, 1]$, it can be used to rank the generated samples from the diffusion model during inference.

Here we have the opportunity to leverage a spatial abstraction different from the one used by the generator. The generator operates on the latent object-centric representation that are suitable to *imagine* possible structures. The discriminator can directly reason about the interactions between the transformed point cloud objects at the point level. To maintain the ability to distinguish each individual object, we add a one-hot encoding to each point feature.

We explore two potential discriminators. The *collision discriminator* learns to predict pairwise collisions between two objects from their partial point clouds. The score of a multi-object structure is computed by averaging the scores for all pairs of objects. Second, the *structure discriminator* learns to classify the validity of the whole multi-object structure. The structure discriminator is also language-conditioned, so it can learn structure-specific constraints. We found that the structure discriminator works better when it is only required to predict if local constraints are satisfied. Therefore, we normalize the scene point cloud and drop parts of the language instruction that specify global constraints such as where to place the structure on the table.

[1]Optionally, we can predict a virtual structure frame and object poses relative to the frame to compute the final object goal poses in the world, similar to prior work [4]

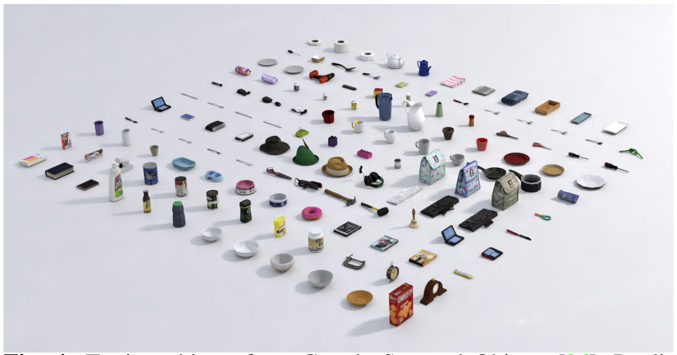

Fig. 4: Testing objects from Google Scanned Objects [36], ReplicaCAD dataset [37], and the YCB Object Set [38]. The test object dataset contains a wide range of textured objects belonging to various classes. None of these objects appear in the training data.

In our preliminary experiments, we found that combining our diffusion model with the collision discriminator is enough to create high-quality samples. Therefore, we only use the structure discriminator for baselines. We further investigated whether a discriminator can be integrated into the diffusion process using a technique called *classifier guidance* [35], but observed no significant benefits. Details are presented in Appendix B.

D. Planning and Inference

In Alg. 1, we show how to combine the different components of our framework to sample object structures. We first initialize a batch of goal poses $\mathbb{R}^{\in B \times N \times (3+3+3)}$ with random noise. We use batch operation on a GPU to efficiently perform diffusion and transform point clouds of multiple objects for different samples. For the discriminators, we also generate point clouds combining all objects after the diffusion process and score them in batches. The ranked samples are returned. Each sample corresponds to a physically and semantically valid multi-object structure that can be used by other components of the manipulation pipeline for planning.

E. Training Details

We train the diffusion model and the discriminators separately. For the diffusion model, we use the dataset from [4] containing high-level language instructions, segmented object point clouds, and sequences of rearrangement actions. We extract the goal poses from the rearrangement actions. We train a single model for all structures where the number of examples for different classes of structures are balanced. We use a batch size of 128 and train the diffusion model on an RTX3090 GPU for about 12 hours. To train the collision discriminator, we randomly sample $100,000$ pairwise configurations for objects

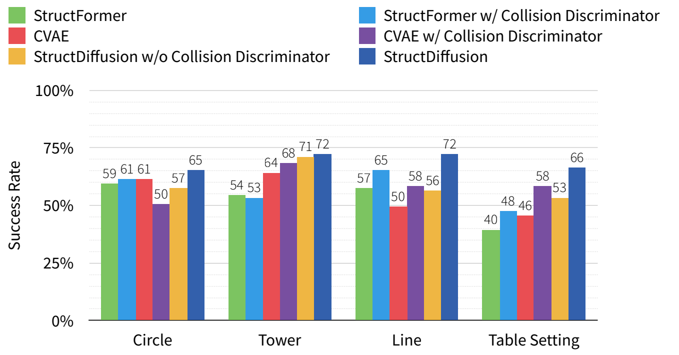

Fig. 5: Success rates for four different classes of structures on held-out objects. Models are evaluated in a physics simulator using unseen objects. A rearrangement is successful only if all objects are placed in physically valid poses and the rearranged scene satisfies the language goal. Compared to StructFormer [4], the model previously proposed for semantic rearrangement, *StructDiffusion* obtains a 16% average improvement in success rate.

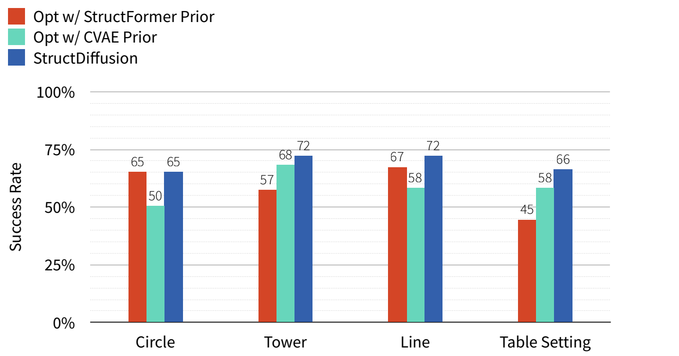

Fig. 6: Comparing *StructDiffusion* with other iterative methods. The two baselines initialize samples of target object poses using either the StructFormer or the CVAE model. The predicted scores of a learned discriminator is then used to guide iterative optimization of the samples. In comparison, *StructDiffusion* directly predicts the noises ϵ_t that need to be removed from the samples at each step.

from the dataset and uses the PyBullet physics simulator [39] to check for collisions. For the structure discriminator, we generate negative examples by randomly perturbing the ground truth target poses ξ_i^{goal} from the dataset without simulating physics. For each negative example, we randomly select a subset of objects to perturb so that the negative examples have different numbers of objects out of place. We augment the data by using point clouds from different time steps of the rearrangement sequence to create the imagined scenes as they usually occlude different objects.

V. Simulation Experiments

We first evaluate our method in simulation by comparing it to existing methods and also a collection of strong baselines we introduce for language-guided multi-object rearrangement.

A. Baselines

We compare our approach against the following baselines:

StructFormer: This prior method uses a multimodal transformer network to generate multi-object structures based on segmented object point clouds and language instructions [4]. The transformer network autoregressively predicts the goal poses of each object. We follow the original work to train a separate model for each class of structure.

Conditional Variational Autoencoder (CVAE): CVAEs have been used to capture different modes for multi-task learning and language-conditioned manipulation [17, 18]. Our CVAE baseline uses the object-centric transformer backbone as a strong baseline for semantic rearrangement. To prevent the latent variable from being ignored when combining the transformer with CVAE, the transformer network predicts the object goal poses in a single forward pass (i.e., not autoregressively). A single model is trained for four classes of structures.

Optimization with Learned Discriminator: This baseline iteratively optimizes the goal poses of objects with the *structure discriminator* that is trained to classify valid rearranged scenes and invalid ones. This general approach has been used extensively for learning language-conditioned manipulation from offline data [40], grasping [41, 42], and predicting stable placements of objects [6], but not for language-conditioned multi-object rearrangement. We use the cross-entropy method for optimization [43], and only optimize the object poses and not the structure pose to simplify the optimization problem. We initialize samples from the baseline generative models because initializing with random values does not lead to meaningful performance.

B. Experimental Setup

We evaluate all models in the PyBullet physics simulator [39]. Point cloud observations are rendered with NViSII [44]. We test on novel object models from both known and unknown categories as our goal is to transfer the model learned in simulation directly to real-world objects. Fig. 4 shows the testing objects, which are collected from Google Scanned Objects [36], ReplicaCAD dataset [37], and the YCB object Set [38]. To generate the test scenes, we use the same data collection pipeline that is used to collect ground truth data from prior work [4]. This ensures that a valid rearrangement can be found for each scene. The set of objects and the language goal for each scene are randomly sampled. Distractor objects are randomly placed in the scene to simulate occlusions.

We report success rate for 100 rearrangements. To isolate the pose prediction problem from other components of the system (e.g., grasp sampling and motion planning), we directly place objects 3cm above the the predicted target poses. A rearrangement is considered as successful if the placements of objects are not preempted due to physics-related failures and the goal scene satisfies all semantic constraints determined by the given language goal. Specifically, we checks for abnormal velocities of objects by running the simulation loop after placing each object. We check possible collisions and intersections between objects using approximate convex decompositions of the 3D object models. We also implement model-based classifiers to evaluate whether the rearrangement satisfy the language goal. For example, we check whether the objects are in a line using the centroids of the models.

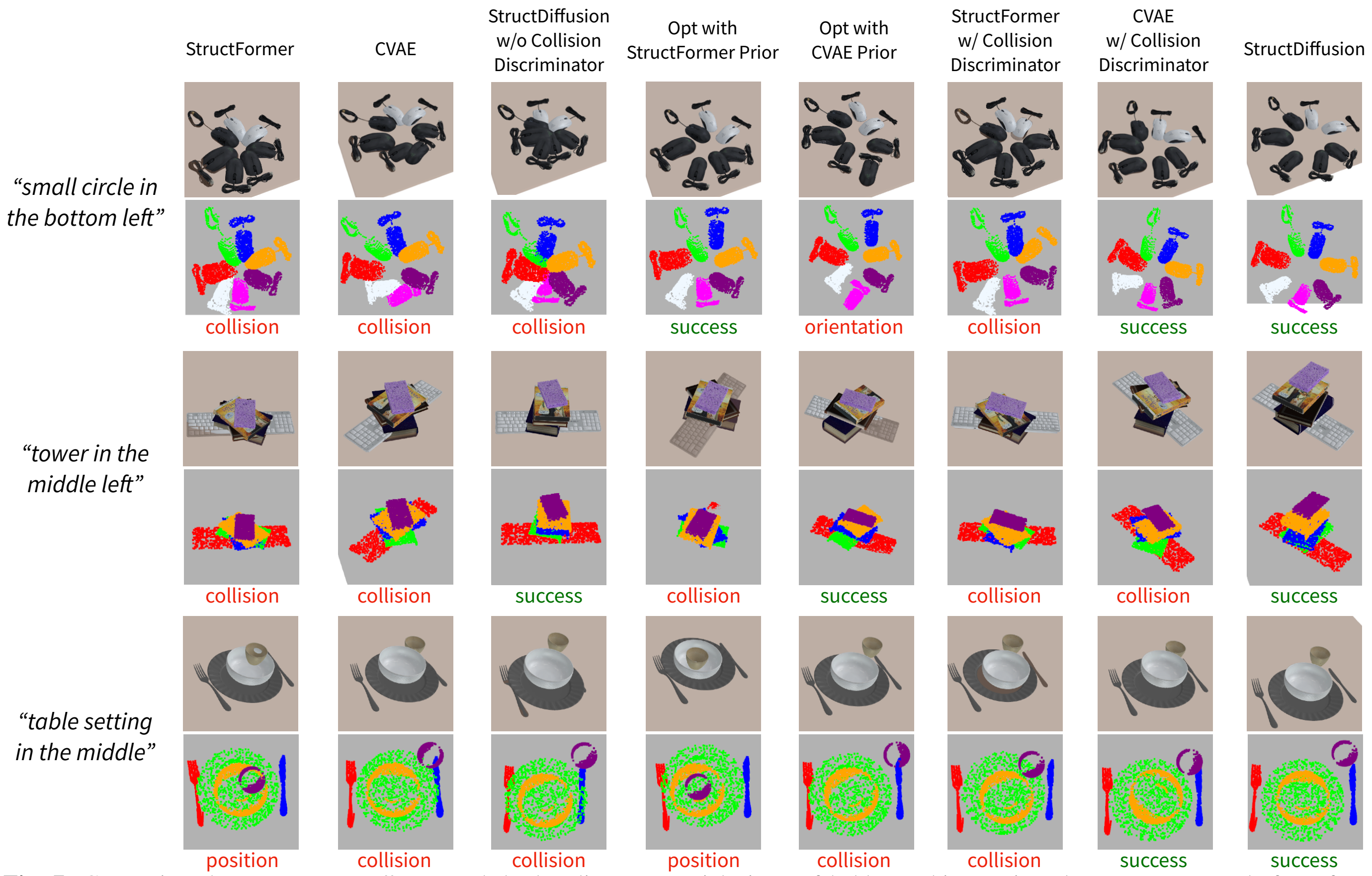

Fig. 7: Comparison between *StructDiffusion* and the baselines on partial views of held-out objects, given language commands from four different categories. *StructDiffusion* is better at resolving constraints involving contact and precise arrangement of objects, avoiding collisions and creating physically realistic placements. The labels indicate whether the structures can be successfully built in the simulation environment and also satisfy the language goal.

C. Comparison with Other Generative Models

In Fig. 5, we compare with other generative models and gain insights into the generator-discriminator design of our model. We see that our complete model, *StructDiffusion*, significantly outperformed all baselines on all structure types. The improvement was most significant for structures that required precise placements of objects and modeling contacts between objects. The generator-discriminator design was necessary because the diffusion model alone still generated invalid samples, especially for the line structures. The performance difference between *StructDiffusion* and the ablated model that does not use discriminator supports that our model can leverage the complementary strengths of object-centric representation and scene-level representation that preserves the point-to-point interactions.

Although applying the collision discriminator also improved the performance of StructFormer and the CVAE, our diffusion model benefited the most from the addition. We attribute this difference to the different diversities of samples from these three classes of generative models. The autoregressive transformer underlying StructFormer does not explicitly model uncertainty, therefore leading to similar samples for each scene. The single source of stochasticity from the latent variable of the CVAE model is also not enough. As the diffusion model incorporates uncertainties at different scales, it has the ability to generate different classes of structures but also generate hypotheses of object placements given only partial, and even heavily occluded, point clouds of objects. We provide a qualitative comparison in Fig. 7. We further break down the failure cases based on structure types and methods to support the insights discussed above in Appendix C.

D. Comparison with Other Iterative Methods

In Fig. 6, we compare *StructDiffusion* with other optimization-based baselines that can take advantage of the additional computational time to iteratively refine the prediction. The result shows that *StructDiffusion* outperformed the other two baselines. Even though strong performance was observed when applying an optimization-based method [6] to other manipulation tasks, we do not see significant benefit in our task. Looking more closely, we observe that the challenging cases that are not yet solved by the non-iterative variants are cases where the placements of objects are highly related. In these cases, the guidance from the discriminator can be ambiguous and leads to local minimal without reaching valid solutions. We hypothesize that leveraging guidance at different scales is necessary.

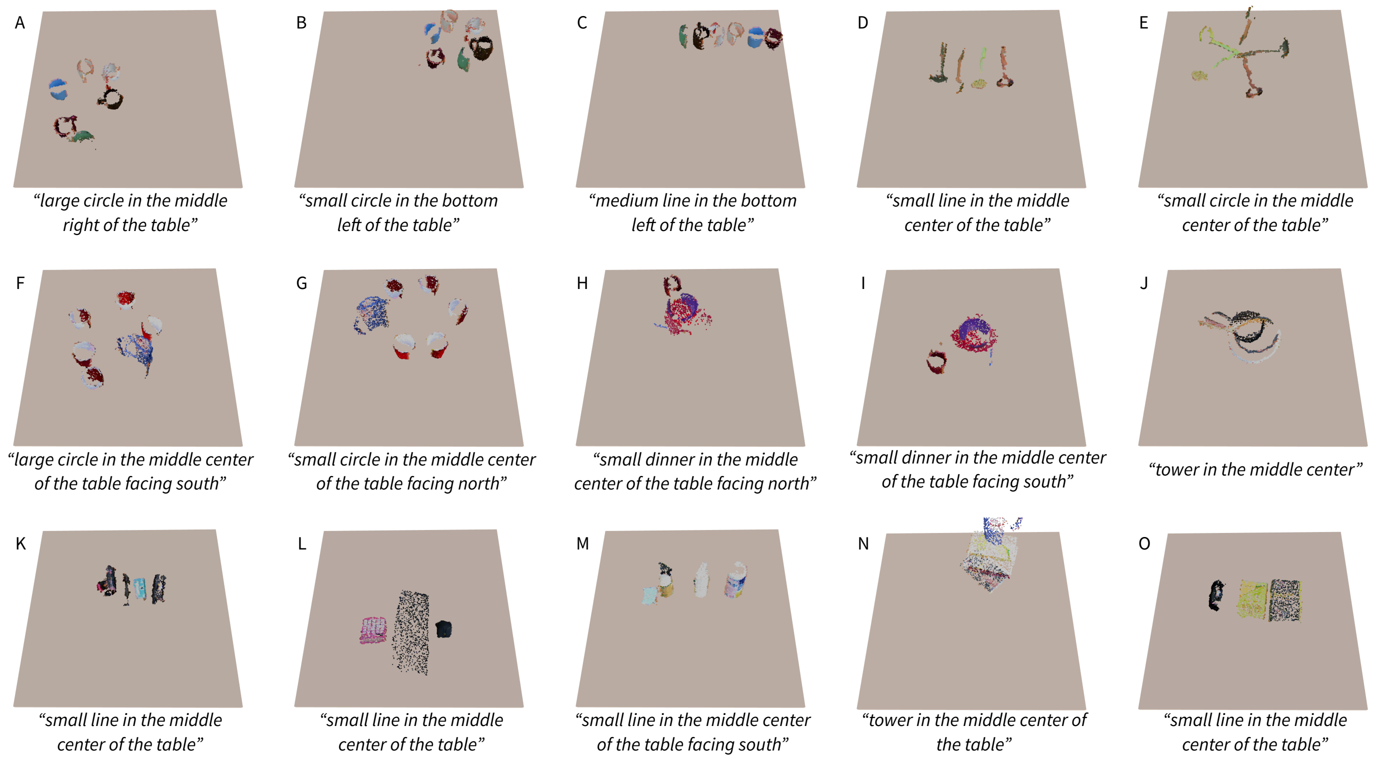
A
"large circle in the middle right of the table"
B
"small circle in the bottom left of the table"
C
"medium line in the bottom left of the table"
D
"small line in the middle center of the table"
E
"small circle in the middle center of the table"
F
"large circle in the middle center of the table facing south"
G
"small circle in the middle center of the table facing north"
H
"small dinner in the middle center of the table facing north"
I
"small dinner in the middle center of the table facing south"
J
"tower in the middle center"
K
"small line in the middle center of the table"
L
"small line in the middle center of the table"
M
"small line in the middle center of the table facing south"
N
"tower in the middle center of the table"
O
"small line in the middle center of the table"

Fig. 8: Examples of predicted structures for real-world objects. We can predict structures from raw point clouds for a wide range of language instructions fitting into four different broad classes. Note the point clouds are incomplete because they were captured from a single camera.

VI. Real World Experiments

In this section, we report on real-world experiments, testing structure assembly on a real robot.

A. Perception and Hardware

We deployed our system on a 7-DoF JACO arm with an Asus Xtion RGB-D Camera. We obtained segmented object point clouds by identifying clusters-of-interest through table surface detection and Euclidean distance clustering, using the Point Cloud Library [45]. For most objects, we calculated antipodal grasps over each object point cloud [46], which are then ordered and executed using pairwise ranking [47]. For objects involved in the table setting arrangements (e.g., forks and plates), we sampled grasps using the Contact-GraspNet [48] because antipodal grasp sampling failed to generate successful grasps for these objects. We used RRT-Connect [49] for motion planning. We released each object 3cm above the predicated target pose for placement.

B. Predictions for Real-World Objects

We first show qualitative examples of the predicted structures for real-world objects in Fig. 8. These examples are created by rigidly transforming the segmented object point clouds from an initial scene with the target poses of the highest ranked structure. Even though our model is trained only on simulation data, it can be directly used to generate semantically diverse and physically valid structures for real-world objects. Our model can generate different variations of the same structure type, as shown in *(A, B)*. The same set of objects can be arranged into completely different classes of structures conditioning on the language, as shown in *(A, C)* and *(D, E)*. Besides changing the positions and sizes of the structures, the orientations of the structures can also be specified in language *(F, G)* and *(H, I)*. Note that even though table settings in the training data are only aligned horizontally as shown in *I*, the use of language and training on other orientation-specific structures enable compositional generalization to a new orientation shown in *H*. Finally, we see non-symmetrical objects (e.g., mugs, knifes, and spatulas) are correctly aligned in *B, D, E, J, H*.

C. Rearrangement with Pick and Place

To reliably rearrange multiple objects given the predicted goals, we combined *StructDiffusion* with grasp and motion planning. We performed nested search to find the target structure to execute. Specifically, we iterate through the generated and ranked structures. For each structure, we sample a set of grasp poses for each object and compute corresponding pre-grasp, standoff, and placement poses based on the prediction. We searched for valid motion plans between these waypoints. If all motion plans have been found, we execute them on the robot.

In Table I, we show success counts and average success rate for trials with different objects and different language goals. For circle, tower, and line structure, valid motion and grasp plans can be found most of the time due to the diverse structures generated by *StructDiffusion*. For table settings, grasp planning is still challenging due to the small tolerance

TABLE I: Robot experiments with real-world objects. We perform each of the task multiple times with different objects and initial placements. We show the number of times that valid grasp and motion plans are found and that the plans are executed successfully by the robot.

Object Categories (#Trials)	Structure	Grasp and Motion Planning	Placement
Bowl, Pan (3)	Small Circle	3	3
Bowl, Pan (3)	Tower	3	2
Bowl, Pan (3)	Small line	2	2
Plate, Spoon, Fork, Knife, Cup (12)	Table Setting	5	4
Overall Success Rate		61.9%	52.4%

of the grasp regions on objects like forks and knifes. The limited diversity of sampled grasps also leads to no valid inverse kinematic solutions in some cases. We observed that partial point clouds due to noisy real sensor and self-occlusions for large objects led to a small number of invalid structure predictions. While planning, we make the assumption that the objects are rigidly attached to the gripper after grasping without slippage. This assumption generally did not hold in the real world and led to occasional failures. This assumption can be relaxed by predicting a post-grasp displacement, using learned models such as [50]. We show examples of successful executions and failure cases in Appendix D.

VII. Conclusions

We introduced *StructDiffusion*, an approach for creating physically-valid structures using multimodal transformers and diffusion models. *StructDiffusion* operates on point cloud images of previously-unseen objects, and can create structures for a range of language instructions.

Specifically, we compared to a wide variety of strong baselines, including the previous state of the art [4] and to a conditional variational autoencoder. End-to-end policies do not perform as well, because they cannot refine placement poses that are *nearly* correct. Using diffusion models for generating diverse samples and a trained discriminator to filter object goal poses significantly improves performance.

In this work, we did not look at optimally planning. In the future, we could look at combining this approach with task and motion planning for unknown objects, as in [25]. Additional experiments presented in Appendix A showed that our model could easily be combined with a pretrained language model to deal with more natural sentences; therefore, we also hope to apply our work to a far wider range of structures and more complex language commands.

Acknowledgements

Weiyu Liu thanks Qinsheng Zhang for initial discussions on diffusion models and gratefully acknowledges support from NSF IIS 1564080 and ONR N00014-16-1-2835. Yilun Du gratefully acknowledges support from NSF grant 2214177; from AFOSR grant FA9550-22-1-0249; from ONR MURI grant N00014-22-1-2740; from ARO grant W911NF-23-1-0034; from the MIT-IBM Watson Lab; and from the MIT Quest for Intelligence.

References

[1] Y. Jiang, A. Gupta, Z. Zhang, G. Wang, Y. Dou, Y. Chen, L. Fei-Fei, A. Anandkumar, Y. Zhu, and L. Fan, "Vima: General robot manipulation with multimodal prompts," *arXiv*, 2022. 1, 2

[2] M. Shridhar, L. Manuelli, and D. Fox, "Cliport: What and where pathways for robotic manipulation," in *CoRL*, 2021. 1, 2

[3] ——, "Perceiver-actor: A multi-task transformer for robotic manipulation," in *CoRL*, 2022. 1, 2

[4] W. Liu, C. Paxton, T. Hermans, and D. Fox, "Structformer: Learning spatial structure for language-guided semantic rearrangement of novel objects," in *ICRA*, 2022. 1, 2, 4, 5, 6, 9

[5] P.-L. Guhur, S. Chen, R. Garcia, M. Tapaswi, I. Laptev, and C. Schmid, "Instruction-driven history-aware policies for robotic manipulations," in *CoRL*, 2022. 1

[6] C. Paxton, C. Xie, T. Hermans, and D. Fox, "Predicting stable configurations for semantic placement of novel objects," in *CoRL*, 2021. 2, 6, 7

[7] M. Janner, Y. Du, J. Tenenbaum, and S. Levine, "Planning with diffusion for flexible behavior synthesis," in *ICML*, 2022. 2

[8] S. Huang, Z. Wang, P. Li, B. Jia, T. Liu, Y. Zhu, W. Liang, and S.-C. Zhu, "Diffusion-based generation, optimization, and planning in 3d scenes," in *CVPR*, 2023. 2

[9] R. Rombach, A. Blattmann, D. Lorenz, P. Esser, and B. Ommer, "High-resolution image synthesis with latent diffusion models," in *CVPR*, 2022. 2, 4

[10] J. Sohl-Dickstein, E. Weiss, N. Maheswaranathan, and S. Ganguli, "Deep unsupervised learning using nonequilibrium thermodynamics," in *ICML*, 2015. 2, 3, 4

[11] J. Ho, A. Jain, and P. Abbeel, "Denoising diffusion probabilistic models," *Advances in Neural Information Processing Systems*, 2020. 2, 3, 4

[12] I. Kapelyukh, V. Vosylius, and E. Johns, "Dall-e-bot: Introducing web-scale diffusion models to robotics," *IEEE Robotics and Automation Letters (RA-L)*, 2023. 2, 4

[13] I. Singh, V. Blukis, A. Mousavian, A. Goyal, D. Xu, J. Tremblay, D. Fox, J. Thomason, and A. Garg, "Progprompt: Generating situated robot task plans using large language models," in *ICRA*, 2023. 2

[14] A. Goyal, A. Mousavian, C. Paxton, Y.-W. Chao, B. Okorn, J. Deng, and D. Fox, "Ifor: Iterative flow minimization for robotic object rearrangement," in *CVPR*, 2022. 2

[15] A. Qureshi, A. Mousavian, C. Paxton, M. Yip, and D. Fox, "Nerp: Neural rearrangement planning for unknown objects," in *RSS*, 2021. 2

[16] M.-H. Guo, J.-X. Cai, Z.-N. Liu, T.-J. Mu, R. R. Martin, and S.-M. Hu, "PCT: Point cloud transformer," *Computational Visual Media*, 2021. 2, 4

[17] C. Lynch, M. Khansari, T. Xiao, V. Kumar, J. Tompson, S. Levine, and P. Sermanet, "Learning latent plans from

play," in *CoRL*, 2020. 2, 6

[18] O. Mees, L. Hermann, and W. Burgard, "What matters in language conditioned robotic imitation learning over unstructured data," *IEEE Robotics and Automation Letters (RA-L)*, 2022. 2, 6

[19] C. Lynch, A. Wahid, J. Tompson, T. Ding, J. Betker, R. Baruch, T. Armstrong, and P. Florence, "Interactive language: Talking to robots in real time," *arXiv*, 2022. 2

[20] A. Brohan, N. Brown, J. Carbajal, Y. Chebotar, J. Dabis, C. Finn, K. Gopalakrishnan, K. Hausman, A. Herzog, J. Hsu *et al.*, "Rt-1: Robotics transformer for real-world control at scale," *arXiv*, 2022. 2

[21] M. Ahn, A. Brohan, N. Brown, Y. Chebotar, O. Cortes, B. David, C. Finn, K. Gopalakrishnan, K. Hausman, A. Herzog *et al.*, "Do as i can, not as i say: Grounding language in robotic affordances," *arXiv*, 2022. 2, 12

[22] B. Chen, F. Xia, B. Ichter, K. Rao, K. Gopalakrishnan, M. S. Ryoo, A. Stone, and D. Kappler, "Open-vocabulary queryable scene representations for real world planning," *arXiv*, 2022. 2

[23] J. Liang, W. Huang, F. Xia, P. Xu, K. Hausman, B. Ichter, P. Florence, and A. Zeng, "Code as policies: Language model programs for embodied control," *arXiv*, 2022. 2, 12

[24] A. Simeonov, Y. Du, B. Kim, F. R. Hogan, J. Tenenbaum, P. Agrawal, and A. Rodriguez, "A long horizon planning framework for manipulating rigid pointcloud objects," in *CoRL*, 2020. 2

[25] A. Curtis, X. Fang, L. P. Kaelbling, T. Lozano-Pérez, and C. R. Garrett, "Long-horizon manipulation of unknown objects via task and motion planning with estimated affordances," in *ICRA*, 2022. 2, 3, 9

[26] A. Bobu, C. Paxton, W. Yang, B. Sundaralingam, Y.-W. Chao, M. Cakmak, and D. Fox, "Learning perceptual concepts by bootstrapping from human queries," *IEEE Robotics and Automation Letters*, 2022. 2

[27] W. Yuan, C. Paxton, K. Desingh, and D. Fox, "Sornet: Spatial object-centric representations for sequential manipulation," in *CoRL*, 2021. 2

[28] A. Simeonov, Y. Du, L. Yen-Chen, , A. Rodriguez, , L. P. Kaelbling, T. L. Perez, and P. Agrawal, "Se(3)-equivariant relational rearrangement with neural descriptor fields," in *CoRL*, 2022. 2

[29] M. Sharma and O. Kroemer, "Relational learning for skill preconditions," *arXiv*, 2020. 2

[30] T. Migimatsu and J. Bohg, "Grounding predicates through actions," in *ICRA*, 2022. 2

[31] J. Urain, N. Funk, G. Chalvatzaki, and J. Peters, "Se(3)-diffusionfields: Learning smooth cost functions for joint grasp and motion optimization through diffusion," in *ICRA*, 2023. 2

[32] A. Ajay, Y. Du, A. Gupta, J. Tenenbaum, T. Jaakkola, and P. Agrawal, "Is conditional generative modeling all you need for decision-making?" *arXiv*, 2022. 2

[33] A. Vaswani, N. Shazeer, N. Parmar, J. Uszkoreit, L. Jones, A. N. Gomez, Ł. Kaiser, and I. Polosukhin, "Attention is all you need," in *Advances in neural information processing systems*, 2017. 2, 3

[34] Y. Zhou, C. Barnes, J. Lu, J. Yang, and H. Li, "On the continuity of rotation representations in neural networks," in *CVPR*, 2019. 5

[35] P. Dhariwal and A. Nichol, "Diffusion models beat gans on image synthesis," *Advances in Neural Information Processing Systems*, 2021. 5

[36] L. Downs, A. Francis, N. Koenig, B. Kinman, R. Hickman, K. Reymann, T. B. McHugh, and V. Vanhoucke, "Google scanned objects: A high-quality dataset of 3d scanned household items," *arXiv*, 2022. 5, 6

[37] A. Szot, A. Clegg, E. Undersander, E. Wijmans, Y. Zhao, J. Turner, N. Maestre, M. Mukadam, D. Chaplot, O. Maksymets, A. Gokaslan, V. Vondrus, S. Dharur, F. Meier, W. Galuba, A. Chang, Z. Kira, V. Koltun, J. Malik, M. Savva, and D. Batra, "Habitat 2.0: Training home assistants to rearrange their habitat," in *Advances in Neural Information Processing Systems*, 2021. 5, 6

[38] B. Calli, A. Singh, A. Walsman, S. Srinivasa, P. Abbeel, and A. M. Dollar, "The ycb object and model set: Towards common benchmarks for manipulation research," in *ICAR*, 2015. 5, 6

[39] E. Coumans and Y. Bai, "Pybullet, a python module for physics simulation in robotics, games and machine learning," 2017. 6

[40] S. Nair, E. Mitchell, K. Chen, S. Savarese, C. Finn *et al.*, "Learning language-conditioned robot behavior from offline data and crowd-sourced annotation," in *CoRL*, 2022. 6

[41] A. Murali, A. Mousavian, C. Eppner, C. Paxton, and D. Fox, "6-dof grasping for target-driven object manipulation in clutter," in *ICRA*, 2020. 6

[42] Q. Lu, M. Van der Merwe, B. Sundaralingam, and T. Hermans, "Multifingered grasp planning via inference in deep neural networks: Outperforming sampling by learning differentiable models," *IEEE Robotics & Automation Magazine*, 2020. 6

[43] M. Chen, S. L. Herbert, H. Hu, Y. Pu, J. F. Fisac, S. Bansal, S. Han, and C. J. Tomlin, "Fastrack: a modular framework for real-time motion planning and guaranteed safe tracking," *IEEE Transactions on Automatic Control*, 2021. 6

[44] N. Morrical, J. Tremblay, Y. Lin, S. Tyree, S. Birchfield, V. Pascucci, and I. Wald, "Nvisii: A scriptable tool for photorealistic image generation," *arXiv*, 2021. 6

[45] R. B. Rusu and S. Cousins, "3d is here: Point cloud library (pcl)," in *ICRA*. IEEE, 2011. 8

[46] A. Ten Pas and R. Platt, "Using geometry to detect grasp poses in 3d point clouds," in *Robotics research*, 2018. 8

[47] D. Kent and R. Toris, "Adaptive autonomous grasp selection via pairwise ranking," in *IROS*, 2018. 8

[48] M. Sundermeyer, A. Mousavian, R. Triebel, and D. Fox, "Contact-graspnet: Efficient 6-dof grasp generation in cluttered scenes," in *ICRA*, 2021. 8

[49] J. J. Kuffner and S. M. LaValle, "RRT-connect: An

efficient approach to single-query path planning," in *ICRA*, 2000. 8

[50] J. Zhao, D. Troniak, and O. Kroemer, "Towards robotic assembly by predicting robust, precise and task-oriented grasps," in *CoRL*, 2022. 9

[51] N. Reimers and I. Gurevych, "Sentence-bert: Sentence embeddings using siamese bert-networks," in *EMNLP*, 2019. 12

Appendix

A. *Towards Natural Language*

In the main experiments, we evaluate the model that encodes word tokens individually. Here, we want to see if our framework can deal with more natural language without predefined vocabularies and at different levels of abstraction (e.g., "make a line" vs "make a short line at the bottom of the table") by combining with a pretrained language model.

1) Language Data: We procedurally generate sentences to train the model. At test time, we leverage sentence embeddings to generalize to new sentences. Given the word tokens in sentences, we first enumerate all possible combinations of the tokens. Note in our definition each token corresponds to a type and a value. For example, [(shape, circle), (size, small), (x_position, center), (y_position, middle), (rotation, south)] can create combinations such as [(shape, circle)], [(size, small), (x_position, center)], [(shape, circle), (x_position, center), (y_position, middle)]. In total, there are 669 unique combinations of word tokens. We then manually created templates for each combination of token types. For example, "build a [shape]", "put the objects into [shape]", and "build a [size] [shape] on the [x_position] of the table facing [rotation]". Combining the enumerated combinations and sentence templates, we generated 3345 unique sentences. We then map all the sentences to pretrained sentence embeddings using a sentence transformer [51], specifically the `all-MiniLM-L6-v2` model. Note that although the generated sentences could have grammar errors, the pretrained sentence transformer should be robust to those errors.

2) Model and Training: We modify the diffusion model to take in a single sentence embedding instead of the embeddings of individual word tokens. The sentence embedding from the pretrained model has a dimension of 384. We use a linear layer to map it to the same dimension as the point cloud embeddings. During training, we randomly sample a combination of the word tokens and map them to predefined sentence embeddings. Therefore, the model should be able to map ambiguous sentences (e.g., build a structure in the middle) to different structures (e.g., a line, a circle, and etc).

3) Inference: We evaluate the performance of the model using fully-specified sentences. As shown in Table A1, we see within 5% decrease in performance across structure types compared to the original model. Leveraging the generalization capability of the pretrained language model, the model should also be able to generalize to sentences not in the rearrangement training data at test time. We show some qualitative examples in Figure A1.

4) Using the Large Language Model to Parse Natural Language: We also explore the prompting techniques [23, 21] to map natural language to word tokens that our original model knows. Examples in Listing 1 shows that this is also a promising direction to bridge the gap between natural language and domain-specific commands.

Listing 1: Example GPT-3 Prompt to map natural language descriptions of target structures to word tokens that our model consumes. Prompt context is in gray, input language descriptions are green, and generated word tokens are purple.

```
Map each natural language instruction about an
object arrangement to available shape, size, and
location. If any element is not specified,
return NONE.

Available shapes: circle, line, table setting, tower
Available size: small, medium, large
Available location: top, middle, bottom

Example: rearrange the objects into a small circle.
Output: circle, small, NONE

Example: put the objects far apart and as a line
on top of the table.
Output: line, large, top

Example: there is a chair near the bottom edge
of the table. Arrange the dishes near the chair.
Output: table setting, NONE, bottom

Example: There is a teapot on the top right corner
of the table. Place the teacups surrounding it.
Output: circle, small, top
```

TABLE A1: Comparing the success rate % in simulation for the two types of language inputs. We observe a small drop in performance when we use a single sentence embedding comparing to individually embed each word tokens for each input sentence.

Language	Circle	Tower	Line	Table Setting
Word Tokens	65	72	72	66
Sentence	63	70	67	67

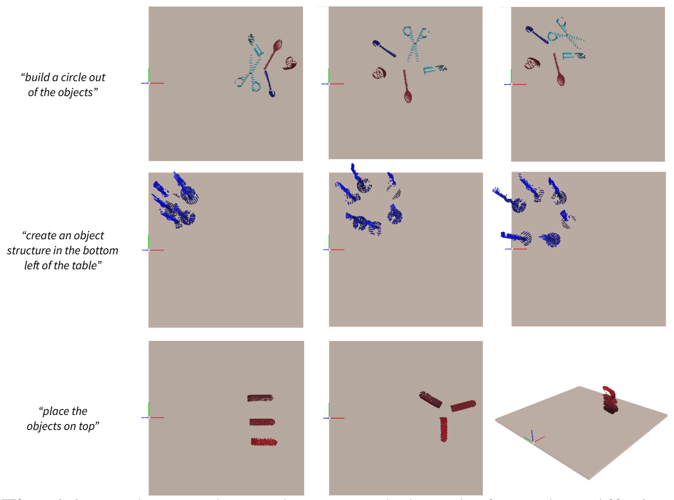
"build a circle out of the objects"
"create an object structure in the bottom left of the table"
"place the objects on top"

Fig. A1: Each row shows three sampled goals from the Diffusion model that is trained with procedurally generated sentences. The model generalizes to input sentences never seen during training by using a pretrained sentence encoder. Because the model is trained on language inputs at different levels of abstractions, the generated samples correspond strongly to structure properties specified in the sentences and at the same time show variations for the properties that are left unspecified.

TABLE A2: The percentage of failure cases due to different types of errors for different models averaged over all structure types.

Model	Intersection	Abnormal Velocity	Not Upright	Semantic Failure
StructDiffusion w/o Collision Discriminator	17.33	14.36	5.20	5.94
StructDiffusion	6.44	17.57	4.46	3.71
CVAE	28.71	14.11	5.20	5.69
CVAE w/ Collision Discriminator	20.05	12.62	3.22	3.47
Opt w/ CVAE Prior	17.33	13.12	5.69	6.93

TABLE A3: The percentage of failure cases due to different types of errors for StructDiffusion.

Structure Type	Intersection	Abnormal Velocity	Not Upright	Semantic Failure
Circle	4.95	24.75	4.95	0.00
Tower	12.87	8.91	4.95	8.91
Line	5.94	17.82	4.95	0.0
Table Setting	1.98	18.81	2.97	5.94

B. *Classifier-Based Collision Guidance*

In addition to utilizing a separate collision discriminator, we may directly integrate a classifier into the underlying sampling procedure of the diffusion model by using classifier based guidance. We present results in Table A4. We find that integrating a noisy collision discriminator with sampling can improve performance for towers and table settings but leads to limited gains for other structures.

C. *Failure Mode Analysis*

We analyze the failure modes for our model based on the simulation experiment. In Table A2, we first compare the number of failure cases in all simulation experiments for different methods. We observe that *StructDiffusion*, which combines a collision discriminator and a diffusion model, drastically reduces errors due to intersections between objects. Comparing CVAE and Optimization with CVAE prior, we also observe that optimizing the goal poses with a learned discriminator can reduce the intersection errors but at the expense of generating more semantically incorrect structures. In Table A3, we further break down the failure modes for our method on different structure types. Building circles tend to have a higher failure rate due to abnormal velocity because large circles may have objects occasionally placed outside of the table. In comparison, towers suffer less from this issue because objects are more closely packed. Reasoning about the environment (e.g., the size of the table) is a necessary next step to address this issue.

D. *Real World Results*

Here we show results from each of the real-world experiments in Table I. Figure A3 shows some additional success examples. Success cases show how StructDiffusion allows us to rearrange previously-unseen objects that did not appear in the training data. Figure A2 includes examples of cases where our method fails. In summary, we see that most of our failures were due to simple motion planning or grasping issues; these could be solved in the future via better integration with task and motion planning algorithms, and with reactive replanning.

TABLE A4: Effect of Collision Classifier Guidance on success rate. This table shows the effect noisy classifier guidance on performance on each of the provided tasks. We do not see clear advantages to using the collision classifier.

	Guidance Weight				
Task	0	1	2	4	8
Circle	65	60	58	58	61
Tower	72	76	74	78	73
Line	72	73	69	73	69
Table Setting	66	70	73	66	70

“short line in the middle and center of the table”

Grasp slippage caused a motion planning failure.

“tower in the middle and center of the table”

Grasp slippage made the predicted goal pose invalid.

“set the table in the center left of the table”

The planned motion failed to avoid another object.

“set the table in the center left of the table”

The grasp failed.

“set the table in the center left of the table”

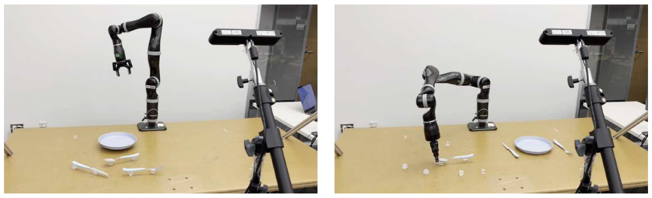

The grasp failed.

“set the table in the center left of the table”

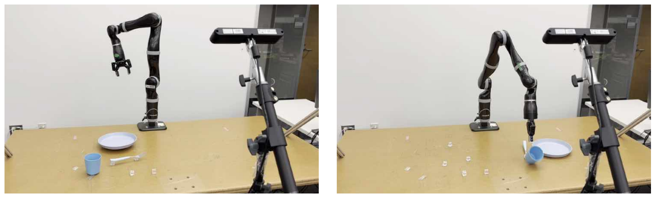

The predict goal does not create enough space between the fork and the cup.

Fig. A2: Real-world failure cases from our robot experiments. A minority of failures come from StructDiffusion; the majority from grasping, planning, and execution failures. This points to future work integrating StructDiffusion with task and motion planning or with

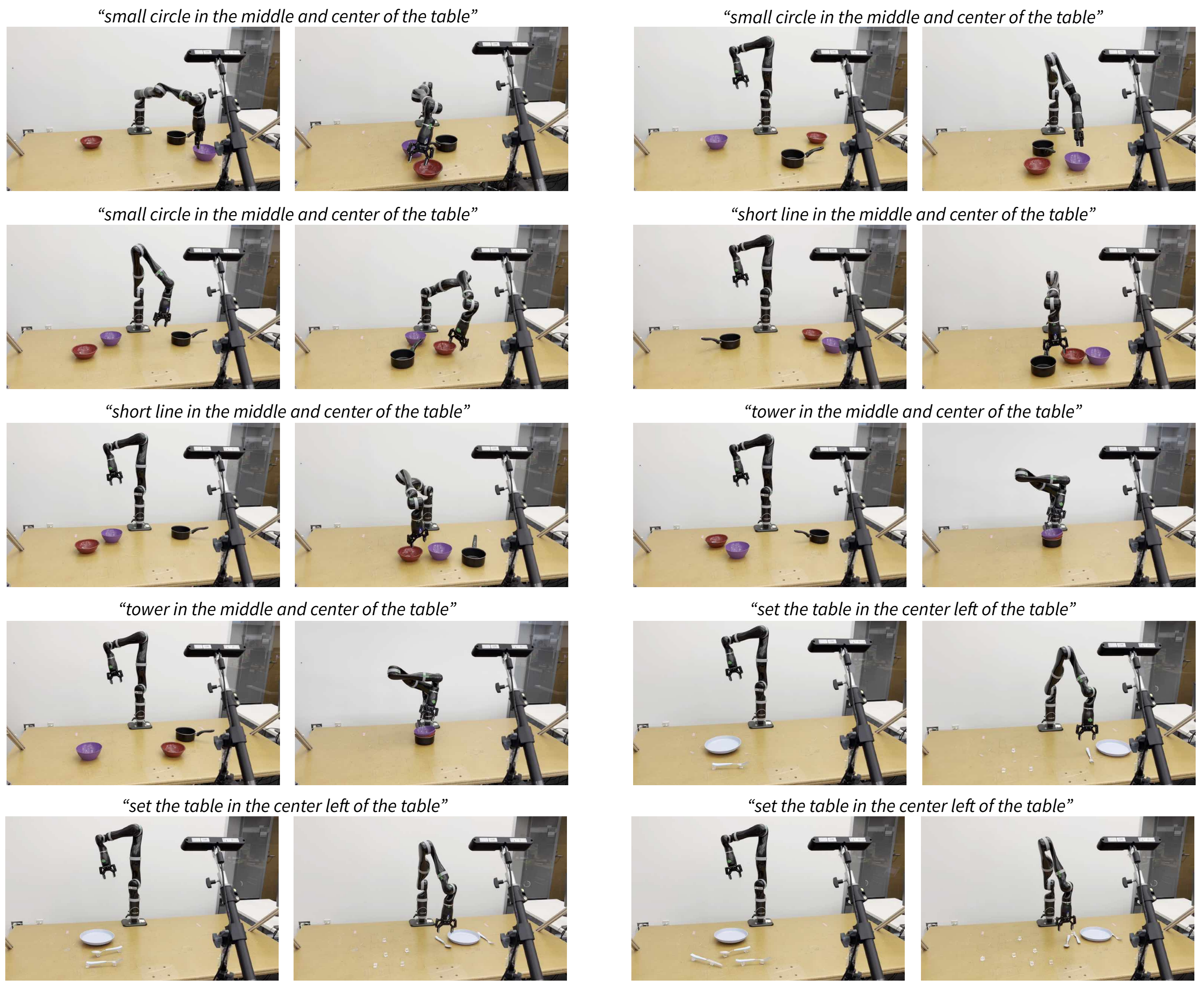
“small circle in the middle and center of the table”
“small circle in the middle and center of the table”
“small circle in the middle and center of the table”
“short line in the middle and center of the table”
“short line in the middle and center of the table”
“tower in the middle and center of the table”
“tower in the middle and center of the table”
“set the table in the center left of the table”
“set the table in the center left of the table”
“set the table in the center left of the table”
Fig. A3: Real-world success cases from our robot experiments. Out of 20 experiments, we saw 11 successes. Most failures were due to grasping and motion planning, not due to issues with our method. All experiments were performed on unseen objects, and StructDiffusion was not trained on any real-world training data.